Microlensing:
Theory, Practice, Results, Future

Lecture 2

Nicholas James Rattenbury

JODRELL BANK CENTRE FOR ASTROPHYSICS
THE UNIVERSITY OF MANCHESTER

Outline of Lectures

Lecture 1: Microlensing History and Theory

Outline of Lectures

Lecture 1: Microlensing History and Theory

- Background
- Motivation/Goals
- Early results
- Evolution of a field
- Basic microlensing theory

Outline of Lectures

Lecture 1: Microlensing History and Theory

Lecture 2: Beyond the Single lens

Outline of Lectures

Lecture 1: Microlensing History and Theory

Lecture 2: Beyond the Single lens

- Finite source star
- Limb Darkening
- Blending
- Parallax
- Xallarap

Single lens lightcurve

The amplification of the source star, at any time t is found using the time-dependent impact parameter:

$$u(t) = \left[{u_{\min}}^2 + \left(\frac{v_\perp \cdot (t - t_0)}{R_E} \right)^2 \right]^{\frac{1}{2}}$$

$$\mu = \frac{u^2 + 2}{u\sqrt{u^2 + 4}}$$

Here $v_\perp$ is the lens transverse velocity with respect to the observer-lens line of sight. $u_{\min}$ is the minimum impact parameter in units of the Einstein radius and t_0 is the time of maximum amplification.

Finite Source effect

The expression above for the amplification of a microlensed star assumes a point-like source.

Finite Source effect

The expression above for the amplification of a microlensed star assumes a point-like source.

This, in general, is not correct as stars are not point-like objects - they have some finite angular size.

Finite Source effect

The expression above for the amplification of a microlensed star assumes a point-like source.

This, in general, is not correct as stars are not point-like objects - they have some finite angular size.

Accounting for the finite source star size is more difficult than assuming a point-like source star, but routines exist to produce lightcurves assuming finite source size.
e.g.

- Witt & Mao, 1994
- Rattenbury et al, 2002
- Dominik, 2007

Finite Source effect

The finite source size effect acts to broaden features. In the case of single lens microlensing, it is clear from an observed broad peak of the event:

Finite Source effect

The finite source size effect acts to broaden features. In the case of single lens microlensing, it is clear from an observed broad peak of the event:

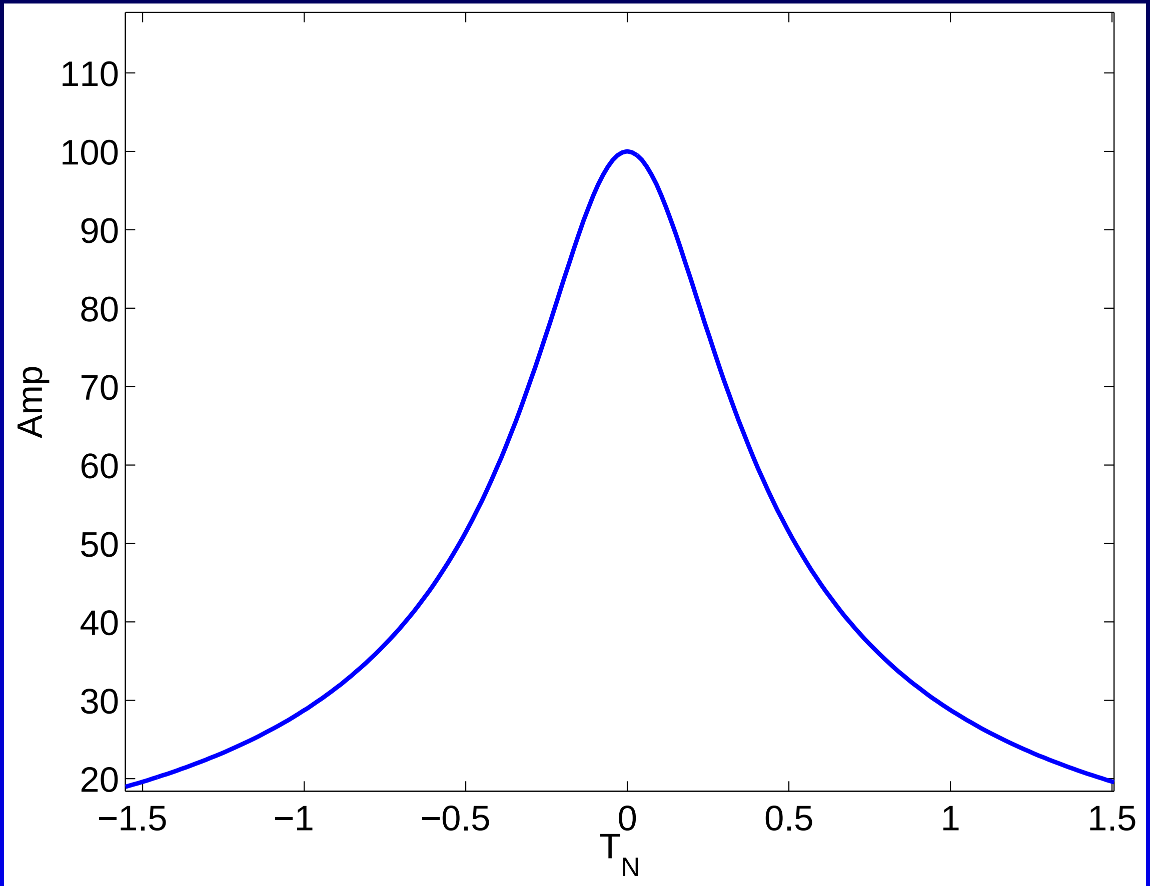

Finite Source effect

The finite source size effect acts to broaden features. In the case of single lens microlensing, it is clear from an observed broad peak of the event:

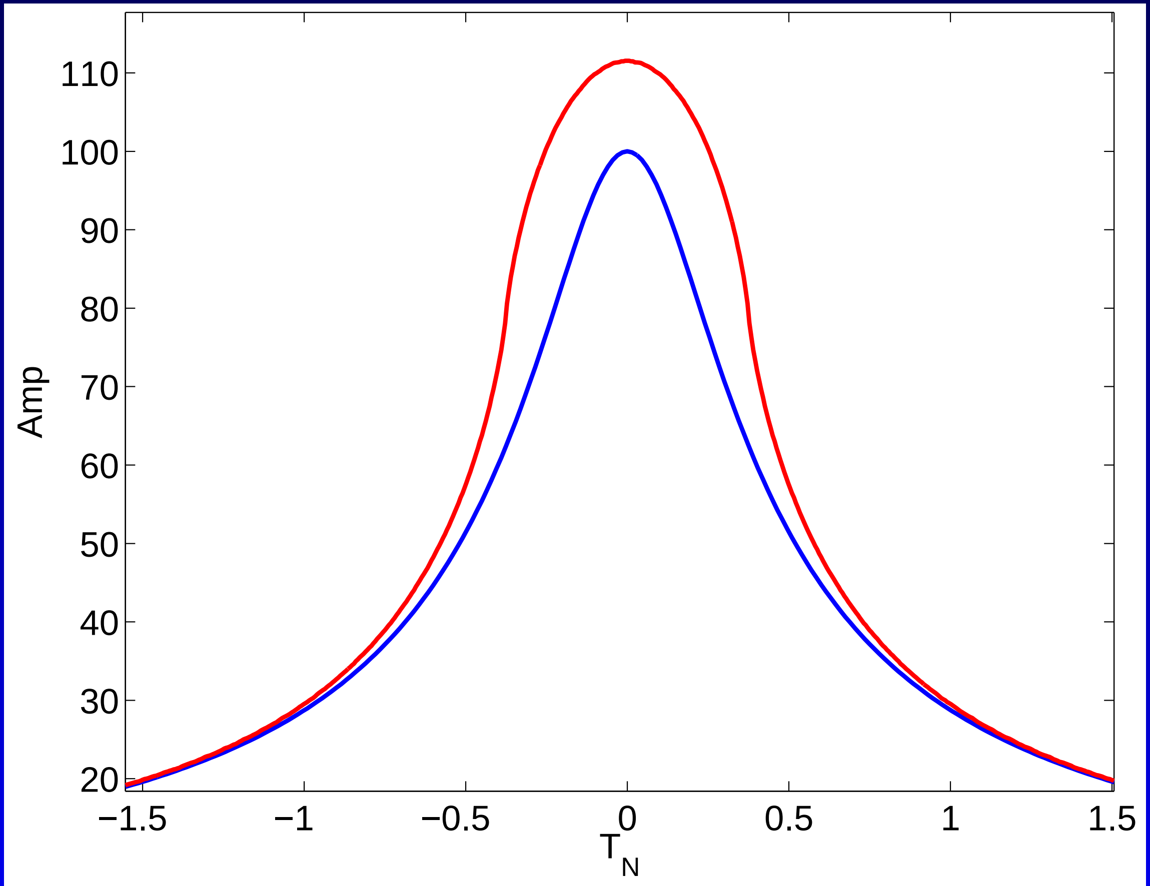

Finite Source effect

The finite source size effect acts to broaden features. In the case of single lens microlensing, it is clear from an observed broad peak of the event:
This effect becomes very important when the gradient of the magnification becomes large, e.g for high amplification events. We shall revisit this later.

Finite Source effect

The finite source size effect acts to broaden features. In the case of single lens microlensing, it is clear from an observed broad peak of the event:
This effect becomes very important when the gradient of the magnification becomes large, e.g for high amplification events. We shall revisit this later.
Finite source size effects have been observed for single events,

- MACHO 95-BLG-30 (Alcock et al 1997)
- OGLE 2003-BLG-262 (Yoo et al 2004)
- OGLE-2003-BLG-238 (Jiang et al)

Finite Source effect

The finite source size effect acts to broaden features. In the case of single lens microlensing, it is clear from an observed broad peak of the event: This effect becomes very important when the gradient of the magnification becomes large, e.g for high amplification events. We shall revisit this later. Finite source size effects have been observed for single events, and for binary lens events:

- 97-BLG-28 (Albrow et al, 1999)
- EROS-BLG-2000-5 (An et al, 2002)
- MOA-2002-BLG-33 (Abe et al 2003)

Finite Source effect

The finite source size effect acts to broaden features. In the case of single lens microlensing, it is clear from an observed broad peak of the event: This effect becomes very important when the gradient of the magnification becomes large, e.g for high amplification events. We shall revisit this later. The source star size is usually expressed as a fraction of the Einstein ring radius:

$$\rho_\star \equiv r_\mathrm{s} = \theta_\mathrm{s}/\theta_\mathrm{E}$$

Finite Source effect

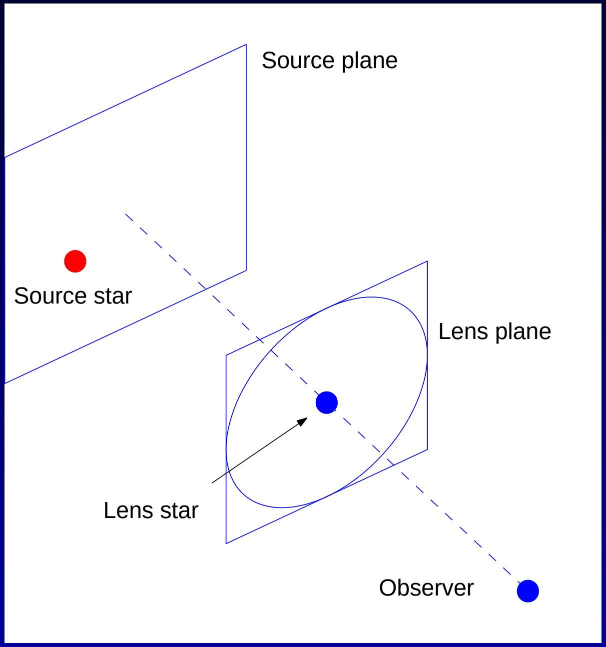

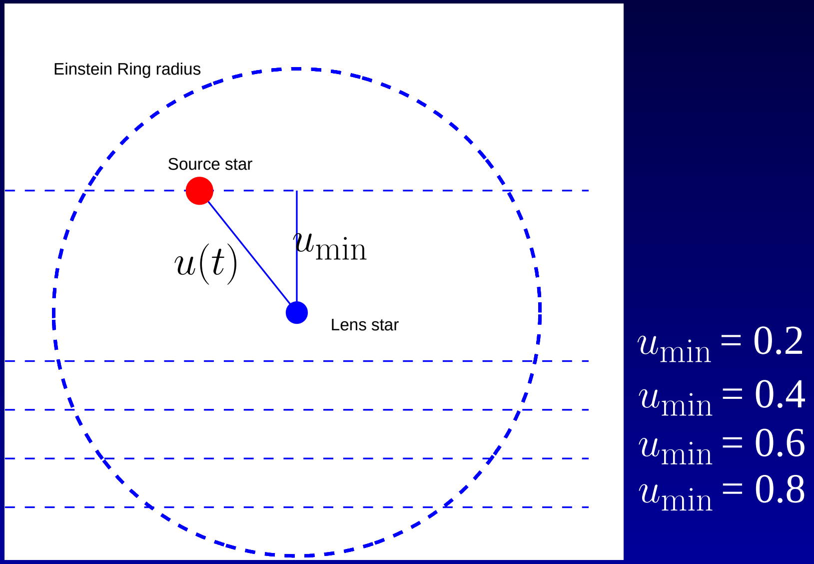

$$R_E = 6.61 \times 10^{11} \sqrt{\frac{M}{0.3 M_\odot}} \sqrt{\frac{D_S}{8\mathrm{kpc}}} \sqrt{(1-d)d} \quad \mathrm{m}$$

Finite Source effect

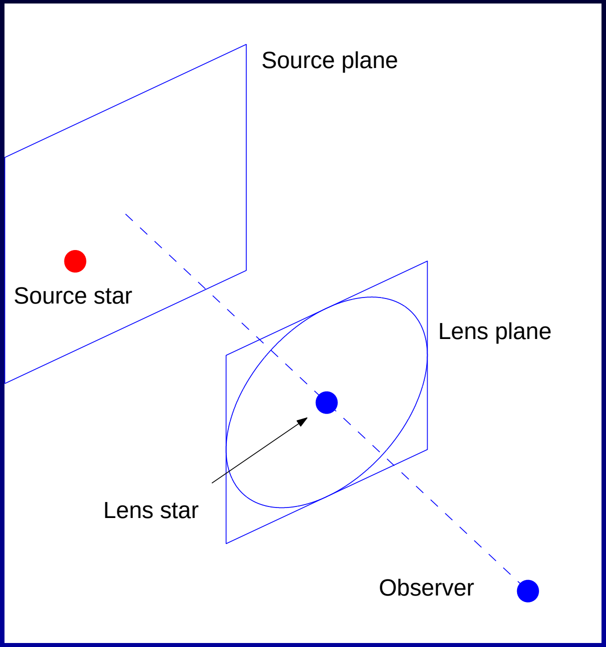

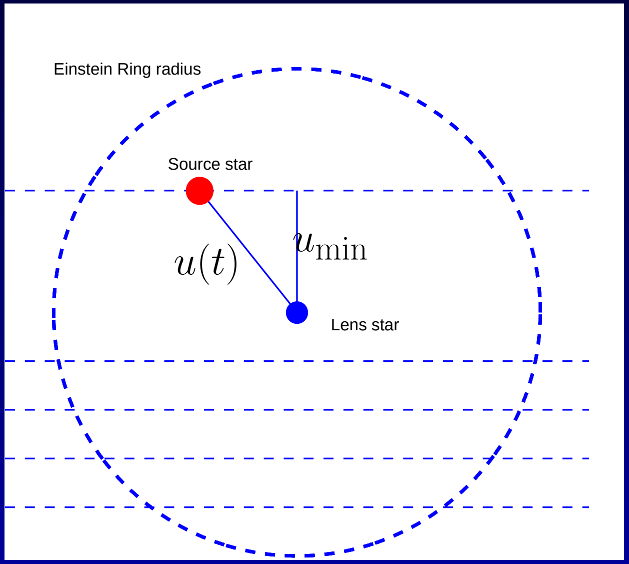

$u_{\min} = 0.2$
$u_{\min} = 0.4$
$u_{\min} = 0.6$
$u_{\min} = 0.8$

$$R'_E = R_E * D_S/D_L$$

Finite Source effect

$$R_E = 6.61 \times 10^{11} \sqrt{\frac{M}{0.3 M_\odot}} \sqrt{\frac{D_S}{8\mathrm{kpc}}} \sqrt{(1-d)d} \quad \mathrm{m}$$

Finite Source effect

$$R_E = 6.61 \times 10^{11} \sqrt{\frac{M}{0.3 M_\odot}} \sqrt{\frac{D_S}{8\mathrm{kpc}}} \sqrt{(1-d)d} \quad \mathrm{m}$$

$$R'_E = R_E * D_S / D_L$$

Finite Source effect

$$R_E \;=\; 6.61 \times 10^{11} \sqrt{\frac{M}{0.3 M_\odot}} \sqrt{\frac{D_S}{8\text{kpc}}} \sqrt{(1-d)d} \quad \text{m}$$

$$R'_E = R_E * D_S / D_L$$

$$r_s = r_\star / R'_E$$

Finite Source effect

$$R_E \;=\; 6.61\times 10^{11}\sqrt{\frac{M}{0.3M_\odot}}\sqrt{\frac{D_S}{8\mathrm{kpc}}}\sqrt{(1-d)d}\quad \mathrm{m}$$

$$R'_E = R_E * D_S/D_L$$

$$r_s = r_\star/R'_E$$

$$r_\odot = 6.96\times 10^8/3.8\times 10^{11}$$

Finite Source effect

$$R_E = 6.61 \times 10^{11} \sqrt{\frac{M}{0.3M_\odot}} \sqrt{\frac{D_S}{8\text{kpc}}} \sqrt{(1-d)d} \quad \text{m}$$

$$R'_E = R_E * D_S / D_L$$

$$r_s = r_\star / R'_E$$

$$r_\odot = 6.96 \times 10^8 / 3.8 \times 10^{11}$$

$$r_\odot \simeq 2 \times 10^{-3}$$

for D_S= 8 kpc, D_L= 6 kpc, M_L= $0.3M_\odot$

Limb Darkening

Stars do not appear as disks of light of uniform brightness.

Limb Darkening

Stars do not appear as disks of light of uniform brightness.

The phenomenon of limb-darkening is the gradual dimming and reddening of light as the star is observed from the centre to the edge of the stellar disk.

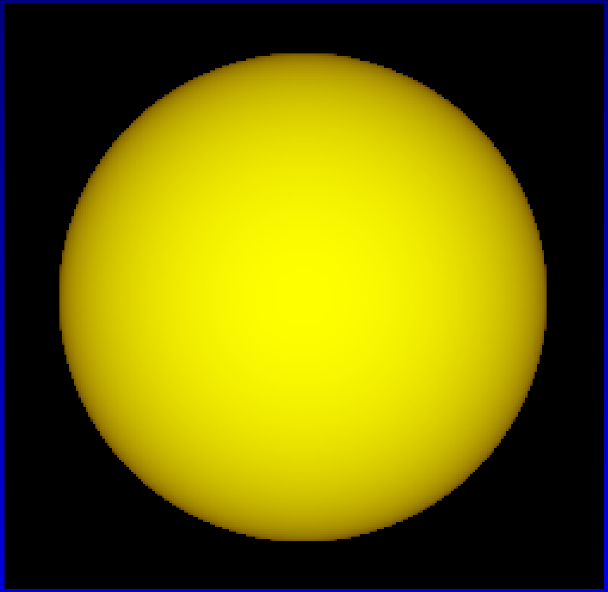

Limb Darkening

Stars do not appear as disks of light of uniform brightness.

The phenomenon of limb-darkening is the gradual dimming and reddening of light as the star is observed from the centre to the edge of the stellar disk.

The light observed from a star is emitted from a constant optical depth; a surface of last scattering. This surface increases in height as the star is observed from the centre to the limb.

Limb Darkening

Stars do not appear as disks of light of uniform brightness.

The phenomenon of limb-darkening is the gradual dimming and reddening of light as the star is observed from the centre to the edge of the stellar disk.

The light observed from a star is emitted from a constant optical depth; a surface of last scattering. This surface increases in height as the star is observed from the centre to the limb.

The temperature of the photosphere decreases with height, therefore the emitted radiation is less intense and longer in wavelength at the limb of the star.

Limb Darkening

Stars do not appear as disks of light of uniform brightness.

The phenomenon of limb-darkening is the gradual dimming and reddening of light as the star is observed from the centre to the edge of the stellar disk.

The light observed from a star is emitted from a constant optical depth; a surface of last scattering. This surface increases in height as the star is observed from the centre to the limb.

The temperature of the photosphere decreases with height, therefore the emitted radiation is less intense and longer in wavelength at the limb of the star.

Limb Darkening

The treatment of limb-darkening is an important element in the analysis of some microlensing events (High amplification, finite source size, caustic crossing).

Limb Darkening

A variety of limb-darkening models exist, along with theoretical values for the model coefficients. The modelling of limb-darkening has progressed from a simple linear model to the more sophisticated models.

Limb Darkening

A variety of limb-darkening models exist, along with theoretical values for the model coefficients. The modelling of limb-darkening has progressed from a simple linear model to the more sophisticated models.

Model	$I(\mu)/I(1)$
Linear	$1 - u(1-\mu)$
Quadratic	$1 - a(1-\mu) - b(1-\mu)^2$
Square root	$1 - c(1-\mu) - d(1-\sqrt{\mu})$
Logarithmic	$1 - e(1-\mu) - f\mu \ln \mu$
Four parameter	$1 - \sum_{k=1}^{4} a_k(1-\mu^{\frac{k}{2}})$

$\mu = cos(\gamma)$

Limb darkening

The linear and square-root limb-darkening models for the Sun.

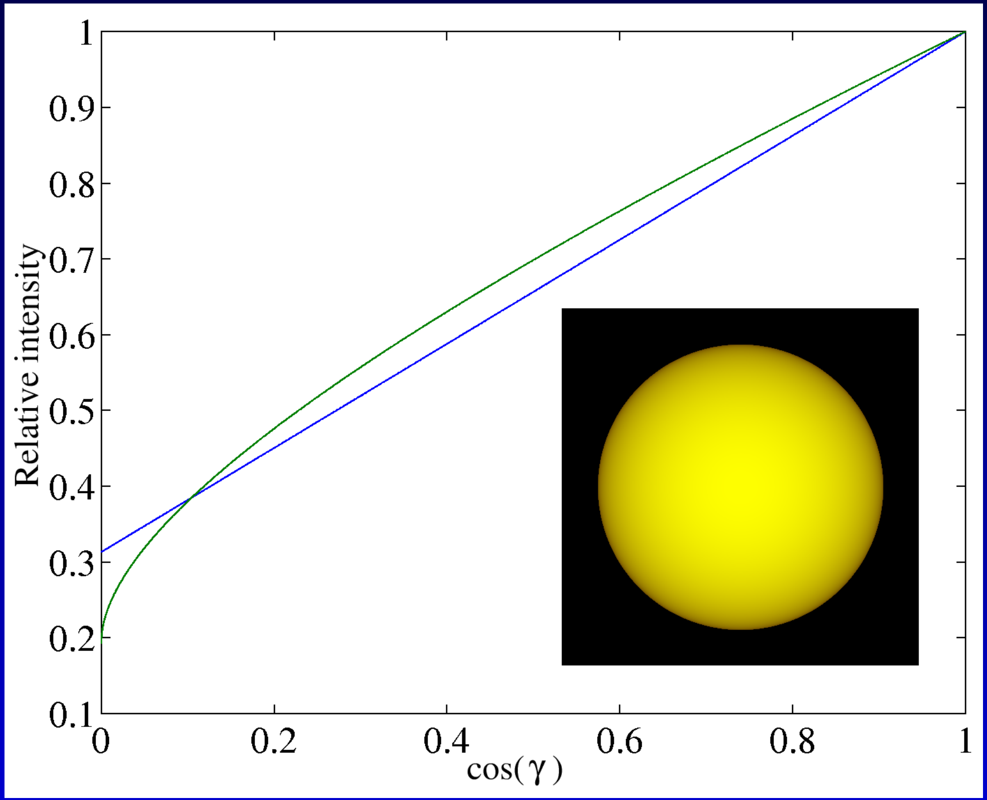

The Sun is a G2V star with $\log g = 4.437$, $T_{\rm eff} = 5777$K, turbulence velocity $v = 1.5{\rm kms}^{-1}$ and [M/H] = 0..

Summary

The finite size of the source star is an important consideration in some single lens events, as is the effect of limb-darkening.

Both these effects can be very important when we start to deal with binary lens events.

We will consider these two source star effects again when we investigate binary lens microlensing.

Blending

A search for microlensing events implicitly requires the observation of millions of stars in order to overcome the intrinsic rarity of the events.

Blending

A search for microlensing events implicitly requires the observation of millions of stars in order to overcome the intrinsic rarity of the events.

By necessity, therefore, crowded stellar fields are the most fruitful hunting grounds for microlensing events.

Blending

A search for microlensing events implicitly requires the observation of millions of stars in order to overcome the intrinsic rarity of the events.

By necessity, therefore, crowded stellar fields are the most fruitful hunting grounds for microlensing events.

Stellar images in such crowded fields often suffer from flux blending, where the profile of one star overlaps that of a neighbour.

Blending

A search for microlensing events implicitly requires the observation of millions of stars in order to overcome the intrinsic rarity of the events.

By necessity, therefore, crowded stellar fields are the most fruitful hunting grounds for microlensing events.

Stellar images in such crowded fields often suffer from flux blending, where the profile of one star overlaps that of a neighbour.

This is a serious problem for the standard photometry procedures, which are based on fitting a profile to every stellar image and integrating the flux under each profile.

Blending

If a stellar profile is contaminated by light from a neighbouring star, this can adversely affect the accuracy to which the star's magnitude can be determined.

Blending

If a stellar profile is contaminated by light from a neighbouring star, this can adversely affect the accuracy to which the star's magnitude can be determined.

The flux observed during a microlensing event is typically a sum of the unlensed flux (the blend flux), F_{u}, and the amplified source (the lensed flux), F_{l}:

Blending

In principle, it is possible to remove, or quantify the effect of blending using difference imaging.

Blending

In principle, it is possible to remove, or quantify the effect of blending using difference imaging.

In practice, crowded field photometry is very difficult, and even the most sophisticated procedures can fail to account for blending.

Blending

In principle, it is possible to remove, or quantify the effect of blending using difference imaging.

In practice, crowded field photometry is very difficult, and even the most sophisticated procedures can fail to account for blending.

Microlensing lightcurves therefore requires in general, two additional fitted flux parameters: $F_{\rm u}$ and $F_{\rm l}$.

Blending

In principle, it is possible to remove, or quantify the effect of blending using difference imaging.

In practice, crowded field photometry is very difficult, and even the most sophisticated procedures can fail to account for blending.

Microlensing lightcurves therefore requires in general, two additional fitted flux parameters: F_{u} and F_{l}.

Blending

Note, however, these two parameters appear as a coefficients of a linear sum:

$$F = F_{\mathrm{l}} \cdot A(u(t)) + F_{\mathrm{u}}$$

and therefore can be solved for using linear least-squares.

Blending

Note, however, these two parameters appear as a coefficients of a linear sum:

$$F = F_{\mathrm{l}} \cdot A(u(t)) + F_{\mathrm{u}}$$

and therefore can be solved for using linear least-squares.

- We will look at lightcurve modelling in Lecture 3
- We will look at difference imaging in Lecture 5

Parallax

In the standard geometry of microlensing events, the velocities of the source star, the lens system and the observer are all considered to be constant during the course of the event.

Parallax

In the standard geometry of microlensing events, the velocities of the source star, the lens system and the observer are all considered to be constant during the course of the event.

Combined with the assumptions that the source star and lens masses are point-like, the simple microlensing equations are valid.

$$F = F_{\mathrm{l}} \cdot A(u(t)) + F_{\mathrm{u}}$$

$$A(u(t)) = \frac{u^2+2}{u\sqrt{u^2+4}} \quad u(t) = \left[{u_{\min}}^2 + \left(\frac{v_\perp \cdot (t-t_0)}{R_E} \right)^2 \right]^{\frac{1}{2}}$$

Parallax

In the standard geometry of microlensing events, the velocities of the source star, the lens system and the observer are all considered to be constant during the course of the event.

Combined with the assumptions that the source star and lens masses are point-like, the simple microlensing equations are valid.

However, the effect of the Earth's orbit around the Sun can be detected in some microlensing events.

Parallax

These parallax events require a more rigorous expression of the time-dependent impact parameter, $u(t)$, taking into account the orbital motion of the Earth.

Parallax

These parallax events require a more rigorous expression of the time-dependent impact parameter, $u(t)$, taking into account the orbital motion of the Earth.

Parallax effects are most likely to be seen in microlensing events of long duration ($t_E \sim 100$ days), as the Earth will move through a significant fraction of its orbit.

Parallax

These parallax events require a more rigorous expression of the time-dependent impact parameter, $u(t)$, taking into account the orbital motion of the Earth.

Parallax effects are most likely to be seen in microlensing events of long duration ($t_E \sim 100$ days), as the Earth will move through a significant fraction of its orbit.

Parallax events have enough information to help break the degeneracy between lens mass, distance and velocity.
(Gould 1992; Alcock et al. 1995)

Parallax

The standard point source, single lens light curve form is given by

$$A(u(t)) = \frac{u^2 + 2}{u\sqrt{u^2 + 4}} \quad u(t) = \left[{u_{\min}}^2 + \left(\frac{v_\perp \cdot (t - t_0)}{R_E} \right)^2 \right]^{\frac{1}{2}}$$

Parallax

The standard point source, single lens light curve form is given by

$$A(u(t)) = \frac{u^2+2}{u\sqrt{u^2+4}} \qquad u(t) = \left[{u_{\min}}^2 + \left(\frac{v_\perp \cdot (t-t_0)}{R_E} \right)^2 \right]^{\frac{1}{2}}$$

To account for the Earth's orbital motion around the Sun, the impact parameter must be modified:

$$\begin{aligned} u(t)^2 &= {u_{\min}}^2 + w(t)^2 + \tilde{r}_\oplus^2 \sin^2\psi \\ &+ 2\tilde{r}_\oplus \sin\psi \left[w(t)\sin\theta + u_{\min}\cos\theta \right] \\ &+ \tilde{r}_\oplus^2 \sin^2\beta \cos^2\psi \\ &+ 2\tilde{r}_\oplus \sin\beta\cos\psi \left[w(t)\cos\theta - u_{\min}\sin\theta \right] \end{aligned}$$

Alcock et al, 1995; Dominik 1998; Mao 1999

Parallax

- θ is the angle between the lens transverse velocity, v, and the projection of the north ecliptic axis onto the lens plane.
- (λ, β): ecliptic co-ordinates.
- $u_{\min}$ is the minimum distance between the lens and the Sun-source line.
- $\tilde{r}_{\oplus} = \frac{1}{\tilde{v} t_E} \left\{1 - \epsilon \cos\left[\Omega_0 (t - t_p)\right]\right\}$
- $\psi = -\phi + \Omega_0 (t - t_p) + 2\epsilon \sin\left[\Omega_0 (t - t_p)\right]$
- $\tilde{v} = \frac{v}{1-x}$ is the lens transverse velocity projected to the solar position and $x = \frac{D_L}{D_S}$.

Parallax

- ϵ: eccentricity of the Earth's orbit
- $\Omega_0 = 2\pi \mathrm{yr}^{-1}$.
- ϕ is the longitude in the ecliptic plane measured from perihelion in the direction of the Earth's motion
- $\phi = \lambda + \pi + \phi_\gamma$
- where ϕ_γ is the longitude of the vernal equinox measured from perihelion, and t_p is the time of perihelion.

Parallax Event MOA-11

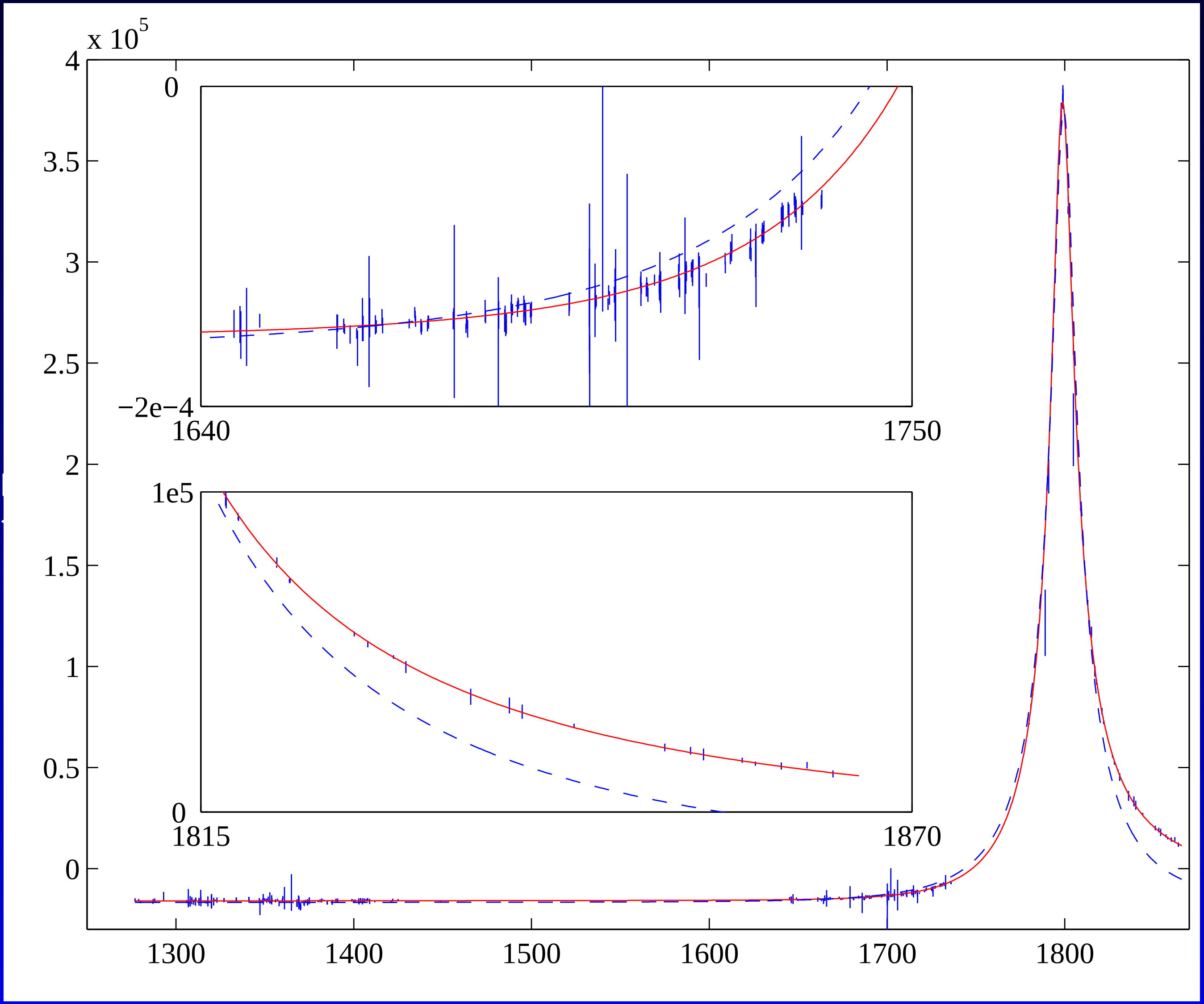

Parallax Event MOA-11

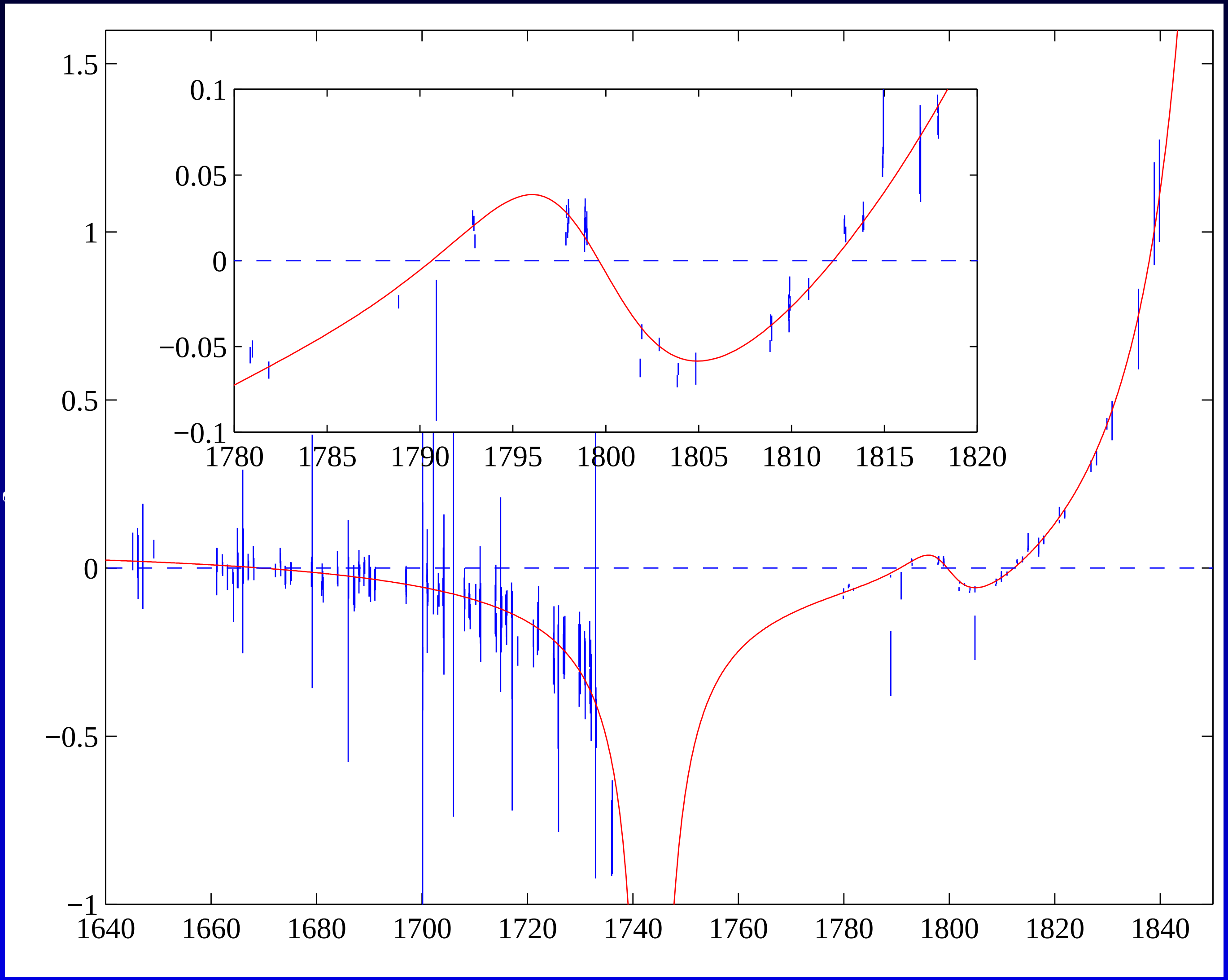

Parallax Event MOA-11

In an ordinary microlensing event, the parameters M_L, $x = \frac{D_L}{D_S}$ and $v_\perp$ are all degenerate: they only affect the Einstein ring crossing time, t_E.

Parallax Event MOA-11

In an ordinary microlensing event, the parameters M_L, $x = \frac{D_L}{D_S}$ and $v_\perp$ are all degenerate: they only affect the Einstein ring crossing time, t_E.

In most cases, the only observable parameter in a microlensing event is $t_E(u_{\min}, t_0)$.

Parallax Event MOA-11

In an ordinary microlensing event, the parameters M_L, $x = \frac{D_L}{D_S}$ and $v_\perp$ are all degenerate: they only affect the Einstein ring crossing time, t_E.

In most cases, the only observable parameter in a microlensing event is $t_E(u_{\min}, t_0)$.

Estimating the parameters of the lens, M_L, $x = \frac{D_L}{D_S}$ and $v_\perp$, becomes one of statistical inference.

Parallax Event MOA-11

In an ordinary microlensing event, the parameters M_L, $x = \frac{D_L}{D_S}$ and $v_\perp$ are all degenerate: they only affect the Einstein ring crossing time, t_E.

In most cases, the only observable parameter in a microlensing event is $t_E(u_{\min}, t_0)$.

Estimating the parameters of the lens, M_L, $x = \frac{D_L}{D_S}$ and $v_\perp$, becomes one of statistical inference.

In a parallax event, however, additional information on the motion of the lens can be established. This allows a more direct estimate of the distance from the observer to the lens, and thereby, an estimate of the lens mass.

Parallax Event MOA-11

Recall the formulae for the Einstein ring radius and crossing time:

$$R_E = \sqrt{\frac{4GM_L D_S x(1-x)}{c^2}} \qquad t_E = \frac{R_E}{v_\perp}$$

Parallax Event MOA-11

Recall the formulae for the Einstein ring radius and crossing time:

$$R_E = \sqrt{\frac{4GM_L D_S x(1-x)}{c^2}} \qquad t_E = \frac{R_E}{v_\perp}$$

In most cases, the lens transverse velocity is set to the most likely rotation speed, that of the Galactic disk rotation: $v_\perp = 220\mathrm{kms}^{-1}$.

Parallax Event MOA-11

Recall the formulae for the Einstein ring radius and crossing time:

$$R_E = \sqrt{\frac{4GM_L D_S x(1-x)}{c^2}} \qquad t_E = \frac{R_E}{v_\perp}$$

In most cases, the lens transverse velocity is set to the most likely rotation speed, that of the Galactic disk rotation: $v_\perp = 220 \mathrm{kms}^{-1}$.
The ratio of the observer-lens and observer-source distances, $x = \frac{D_L}{D_S}$, is similarly estimated with D_L= 6 kpc and D_S= 8kpc.

Parallax Event MOA-11

With parallax events, we learn about the lens star motion.

$$R_E = \sqrt{\frac{4GM_L D_S x(1-x)}{c^2}} \qquad t_E = \frac{R_E}{v_\perp}$$

Parallax Event MOA-11

With parallax events, we learn about the lens star motion.

$$R_E = \sqrt{\frac{4GM_L D_S x(1-x)}{c^2}} \qquad t_E = \frac{R_E}{v_\perp}$$

Substituting $v = \tilde{v}(1-x)$ yields (Mao 1999):

$$M_L(x) = \frac{1-x}{x}\frac{\tilde{v}^2 t_E^2 c^2}{4GD_S} \qquad \text{(-4)}$$

Parallax Event MOA-11

With parallax events, we learn about the lens star motion.

$$R_E = \sqrt{\frac{4GM_L D_S x(1-x)}{c^2}} \qquad t_E = \frac{R_E}{v_\perp}$$

Substituting $v = \tilde{v}(1-x)$ yields (Mao 1999):

$$M_L(x) = \frac{1-x}{x}\frac{\tilde{v}^2 t_E^2 c^2}{4GD_S} \qquad \text{(-4)}$$

Parameters $\tilde{v}$ and t_E can be obtained through non-linear fitting.

Parallax Event MOA-11

With parallax events, we learn about the lens star motion.

$$R_E = \sqrt{\frac{4GM_L D_S x(1-x)}{c^2}} \qquad t_E = \frac{R_E}{v_\perp}$$

Substituting $v = \tilde{v}(1-x)$ yields (Mao 1999):

$$M_L(x) = \frac{1-x}{x}\frac{\tilde{v}^2 t_E^2 c^2}{4GD_S} \qquad \text{(-4)}$$

A good estimate for the source distance is D_S= 8 kpc, although a more rigorous treatment can be obtained through an analysis of the source star colour.

Parallax Event MOA-11

With parallax events, we learn about the lens star motion.

$$R_E = \sqrt{\frac{4GM_L D_S x(1-x)}{c^2}} \qquad t_E = \frac{R_E}{v_\perp}$$

Substituting $v = \tilde{v}(1-x)$ yields (Mao 1999):

$$M_L(x) = \frac{1-x}{x}\frac{\tilde{v}^2 t_E^2 c^2}{4GD_S} \tag{-4}$$

What remains to be determined is the distance ratio x.

Parallax Event MOA-11

Using a simple expression for observed lens velocity as a function of distance ratio:

$$\tilde{v} = \frac{220x}{1-x} \quad \mathrm{kms}^{-1}$$

Parallax Event MOA-11

Using a simple expression for observed lens velocity as a function of distance ratio:

$$\tilde{v} = \frac{220x}{1-x} \quad \mathrm{kms}^{-1}$$

we get for MOA-11 $x \simeq 0.18$ and $D_L = xD_S \simeq 1.4$ kpc.

Parallax Event MOA-11

Using a simple expression for observed lens velocity as a function of distance ratio:

$$\tilde{v} = \frac{220x}{1-x} \quad \text{kms}^{-1}$$

we get for MOA-11 $x \simeq 0.18$ and $D_L = xD_S \simeq 1.4$ kpc.
Using the fitted parameters for MOA-11, we obtain the following lens mass:

$$M_L(x) = 0.065 M_\odot \frac{1-x}{x}$$

With $x = 0.18$, the lens mass is $M_L \simeq 0.011 M_\odot$.

Parallax Event MOA-11

A more thorough estimate of the lens mass assumes Galactic population dynamics and can be determined through the likelihood function of Alcock (1995):

Parallax Event MOA-11

A more thorough estimate of the lens mass assumes Galactic population dynamics and can be determined through the likelihood function of Alcock (1995):

$$L(x|\tilde{v}) \propto \sqrt{x(1-x)}\rho_L(x)\tilde{v}(1-x)^3 \int f_S(v_S) f_L(v_L) dv_S$$

Parallax Event MOA-11

A more thorough estimate of the lens mass assumes Galactic population dynamics and can be determined through the likelihood function of Alcock (1995):

$$L(x|\tilde{v}) \propto \sqrt{x(1-x)}\rho_L(x)\tilde{v}(1-x)^3 \int f_S(v_S) f_L(v_L) dv_S$$

where $\rho_L(x)$ is the density of lenses at distance x (Used Bahcall 1986).

Parallax Event MOA-11

A more thorough estimate of the lens mass assumes Galactic population dynamics and can be determined through the likelihood function of Alcock (1995):

$$L(x|\tilde{v}) \propto \sqrt{x(1-x)}\rho_L(x)\tilde{v}(1-x)^3 \int f_S(v_S)f_L(v_L)dv_S$$

The functions f_S and f_L are the two-dimensional velocity distribution functions.

Parallax Event MOA-11

A more thorough estimate of the lens mass assumes Galactic population dynamics and can be determined through the likelihood function of Alcock (1995):

$$L(x|\tilde{v}) \propto \sqrt{x(1-x)}\rho_L(x)\tilde{v}(1-x)^3 \int f_S(v_S) f_L(v_L) dv_S$$

The lens velocity can be expressed as:
$v_L = (1-x)(v_\odot + \tilde{v}) + xv_S$, where $v_\odot$ is the velocity of the Sun, $v_\odot = 220\mathrm{kms}^{-1}$.

Parallax Event MOA-11

A more thorough estimate of the lens mass assumes Galactic population dynamics and can be determined through the likelihood function of Alcock (1995):

$$L(x|\tilde{v}) \propto \sqrt{x(1-x)}\rho_L(x)\tilde{v}(1-x)^3 \int f_S(v_S) f_L(v_L) dv_S$$

The non-rotating barred bulge Galactic model of Han (1995) was used for the functions f_S and f_L. For simplicity, the source was assumed to reside in the bulge and the lens in the disk.

Parallax Event MOA-11

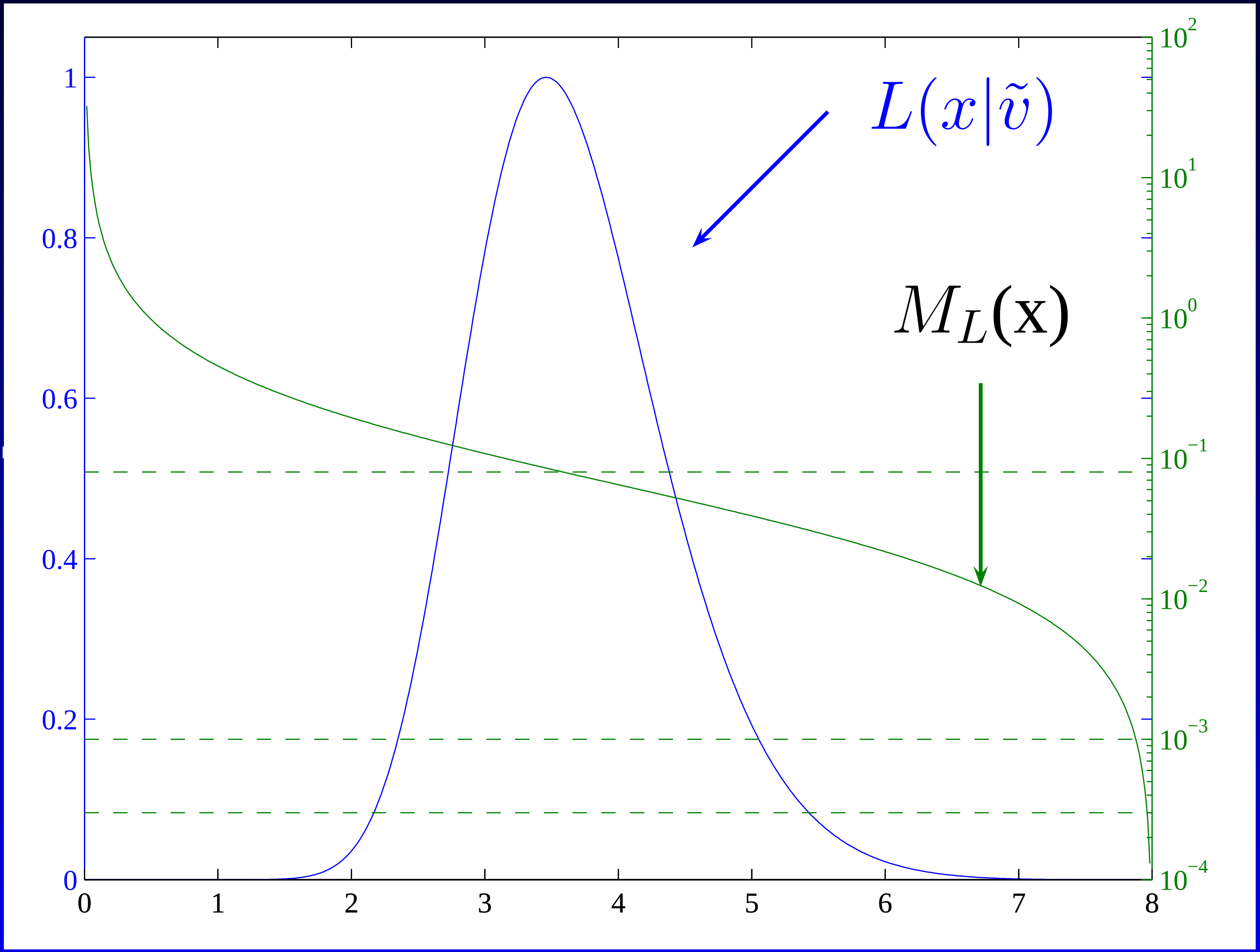

Parallax Event MOA-11

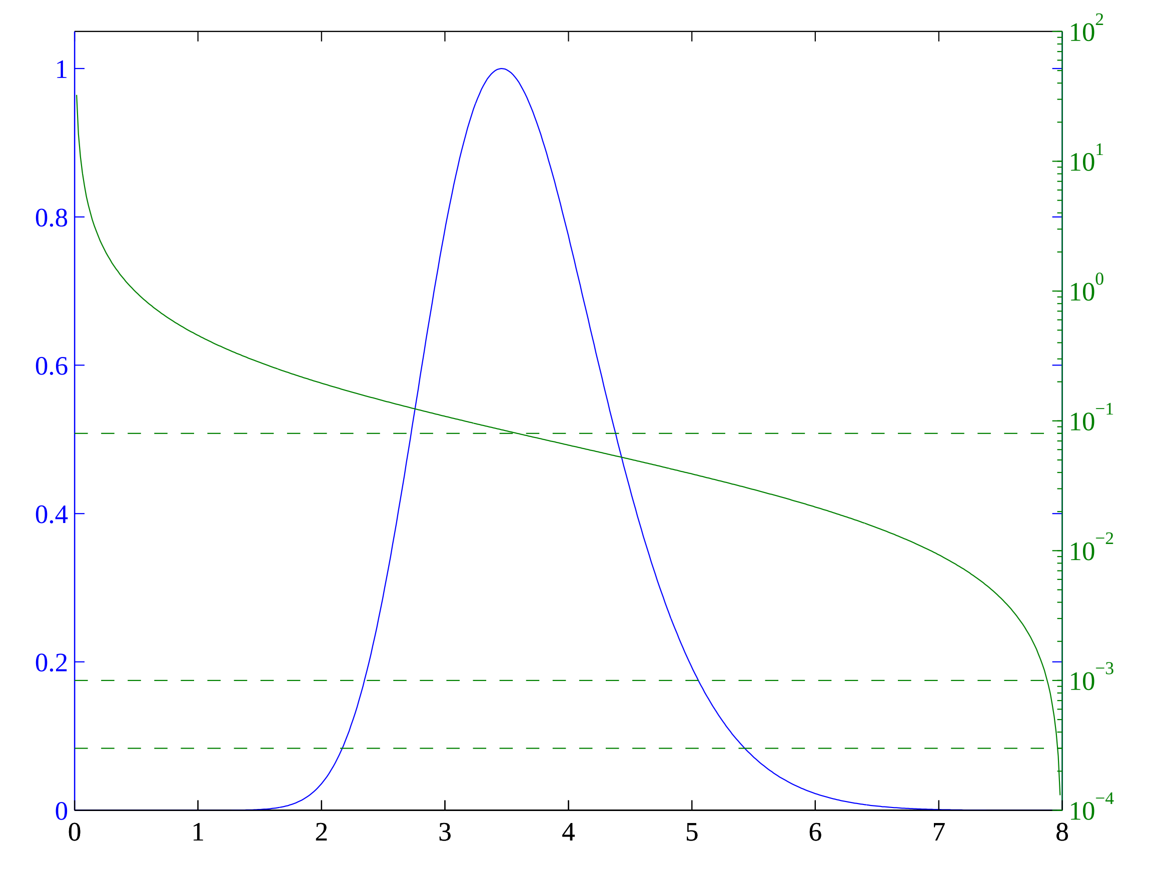

The most likely lens mass distance is at $D_L = xD_S = 0.432D_S = 3.46$ kpc. This corresponds to a likely lens mass of $M_L \simeq 0.086M_\odot$. Interestingly, this value is just above that of a brown dwarf object.

Parallax Event MOA-11

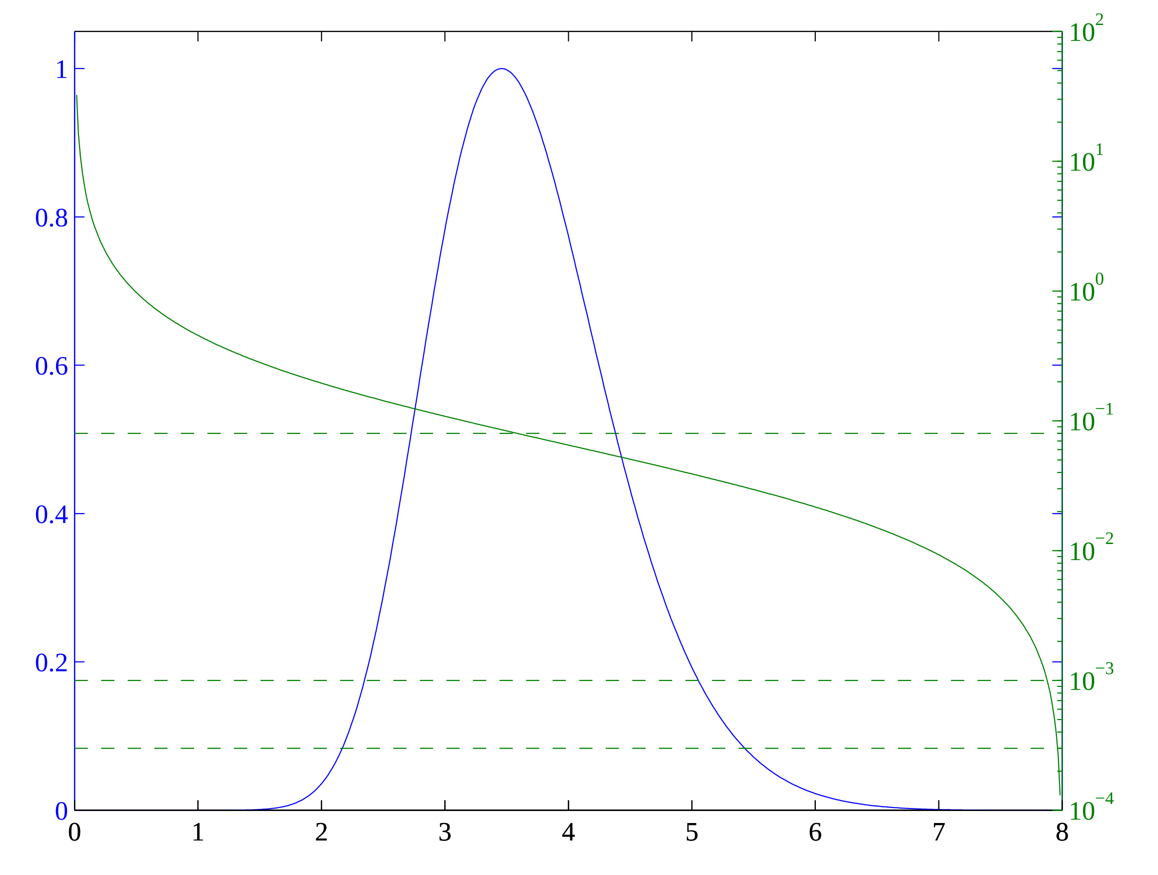

The most likely lens mass distance is at $D_L = xD_S = 0.432D_S = 3.46$ kpc. This corresponds to a likely lens mass of $M_L \simeq 0.086M_\odot$. Interestingly, this value is just above that of a brown dwarf object.

See also papers by e.g. Gould; Dominik; Smith

Xallarap

Xallarap is the effect of a binary source system. The source star is in orbit around another star, and gives a signature analagous to parallax (Griest & Hu 1992).

Xallarap

Xallarap is the effect of a binary source system. The source star is in orbit around another star, and gives a signature analagous to parallax (Griest & Hu 1992).

- Xallarap appears as periodic modulation in the light curve

Xallarap

Xallarap is the effect of a binary source system. The source star is in orbit around another star, and gives a signature analagous to parallax (Griest & Hu 1992).

- Xallarap appears as periodic modulation in the light curve
- Allows a fit to the semimajor axis of the binary source (in units of R'_E)

Xallarap

Xallarap is the effect of a binary source system. The source star is in orbit around another star, and gives a signature analagous to parallax (Griest & Hu 1992).

- Xallarap appears as periodic modulation in the light curve
- Allows a fit to the semimajor axis of the binary source (in units of R'_E)
- Estimating the physical semimajor axis allows an estimate of R_E

Xallarap

Xallarap is the effect of a binary source system. The source star is in orbit around another star, and gives a signature analagous to parallax (Griest & Hu 1992).

- Xallarap appears as periodic modulation in the light curve
- Allows a fit to the semimajor axis of the binary source (in units of R'_E)
- Estimating the physical semimajor axis allows an estimate of R_E
- Combined with a measurement of t_E, we can start to break the degeneracy between the three degenerate parameters lens parameters mass, distance, and transverse velocity.

Xallarap

- The binary source orbital period $P_{\rm s} \lesssim t_E$.

Xallarap

- The binary source orbital period $P_{\rm s} \lesssim t_E$.
  - This is so that the sources move through their orbits during the time they are microlensed by a significant amount and and $P_{\rm s}$ may be determined.

Xallarap

- The binary source orbital period $P_{\rm s} \lesssim t_E$.
- The orbital separation of the sources $a_{\rm s} \gtrsim R'_E$

Xallarap

- The binary source orbital period $P_{\rm s} \lesssim t_E$.
- The orbital separation of the sources $a_{\rm s} \gtrsim R'_E$
  - If $a_{\rm s} \ll R'_E$ the two sources appear to be essentially a single object.
  - This means the xallarap effect is more likely to be detected for events where the lens is close to the sources.
  - Similarly the parallax effect is most easily detected when the lens is relatively close to the Sun-Earth system.

Xallarap

- The binary source orbital period $P_{\rm s} \lesssim t_E$.
- The orbital separation of the sources $a_{\rm s} \gtrsim R'_E$
- See Dominik (1998) for more details on parallax and xallarap

Xallarap

- The binary source orbital period $P_{\rm s} \lesssim t_E$.
- The orbital separation of the sources $a_{\rm s} \gtrsim R'_E$
- See Dominik (1998) for more details on parallax and xallarap
- Alcock et al (2001) measured the xallarap effect for MACHO 96-LMC-2

Xallarap

Alcock et al, 2001, ApJ, 552:259-267

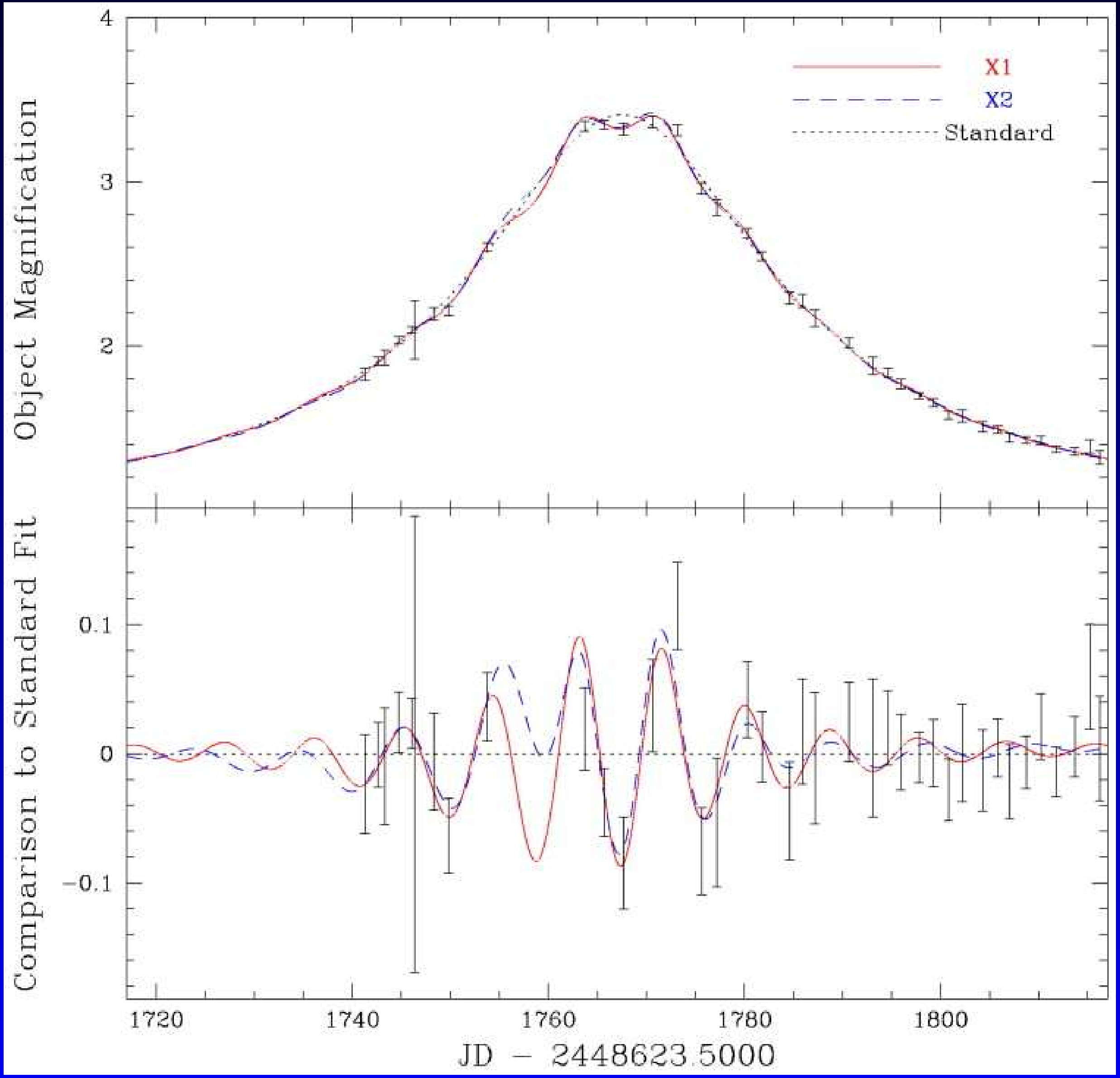

Xallarap

- From source colour, estimate source mass. Find mass of companion via modelling.

Xallarap

- From source colour, estimate source mass. Find mass of companion via modelling.
- With the total source system mass and orbital period, can find source orbit radius in absolute units (i.e. AU).

Xallarap

- From source colour, estimate source mass. Find mass of companion via modelling.
- With the total source system mass and orbital period, can find source orbit radius in absolute units (i.e. AU).
- The xallarap fit parameter relates the binary's semimajor axis in units of R'_E

Xallarap

- From source colour, estimate source mass. Find mass of companion via modelling.
- With the total source system mass and orbital period, can find source orbit radius in absolute units (i.e. AU).
- The xallarap fit parameter relates the binary's semimajor axis in units of R'_E
- Now have source orbit radius in absolute units, and in units of R'_E, therefore can find R_E in absolute units.

Xallarap

- From source colour, estimate source mass. Find mass of companion via modelling.
- With the total source system mass and orbital period, can find source orbit radius in absolute units (i.e. AU).
- The xallarap fit parameter relates the binary's semimajor axis in units of R'_E
- Now have source orbit radius in absolute units, and in units of R'_E, therefore can find R_E in absolute units.
- Then have a measurement of the lens proper motion $\mu = \frac{v_\perp}{D_L} = \frac{R'_E}{t_E D_S}$

Xallarap

- From source colour, estimate source mass. Find mass of companion via modelling.
- With the total source system mass and orbital period, can find source orbit radius in absolute units (i.e. AU).
- The xallarap fit parameter relates the binary's semimajor axis in units of R'_E
- Now have source orbit radius in absolute units, and in units of R'_E, therefore can find R_E in absolute units.
- Then have a measurement of the lens proper motion $\mu = \frac{v_\perp}{D_L} = \frac{R'_E}{t_E D_S}$
- Solution for lens mass similar to that for parallax